JOURNAL OF VIROLOGY, Dec. 2011, p. 12227–12240 Vol. 85, No. 23
0022-538X/11/$12.00 doi:10.1128/JVI.00716-11

Lethal Mutagenesis of Foot-and-Mouth Disease Virus Involves Shifts in Sequence Space▽†

Celia Perales,[1,2] Michel Henry,[3] Esteban Domingo,[1,2] Simon Wain-Hobson,[3] and Jean-Pierre Vartanian[3]*

Centro de Biología Molecular Severo Ochoa (CSIC-UAM), Consejo Superior de Investigaciones Científicas (CSIC), Campus de Cantoblanco, 28049 Madrid, Spain[1]; Centro de Investigación Biomédica en Red de Enfermedades Hepáticas y Digestivas (CIBERehd), Barcelona, Spain[2]; and Unité de Rétrovirologie Moléculaire, Institut Pasteur, 28 Rue du Dr. Roux, 75724 Paris Cedex 15, France[3]

Received 8 April 2011/Accepted 29 August 2011

Lethal mutagenesis or virus transition into error catastrophe is an antiviral strategy that aims at extinguishing a virus by increasing the viral mutation rates during replication. The molecular basis of lethal mutagenesis is largely unknown. Previous studies showed that a critical substitution in the foot-and-mouth disease virus (FMDV) polymerase was sufficient to allow the virus to escape extinction through modulation of the transition types induced by the purine nucleoside analogue ribavirin. This substitution was not detected in mutant spectra of FMDV populations that had not replicated in the presence of ribavirin, using standard molecular cloning and nucleotide sequencing. Here we selectively amplify and analyze low-melting-temperature cDNA duplexes copied from FMDV genome populations passaged in the absence or presence of ribovirin Hypermutated genomes with high frequencies of A and U were present in both ribavirin -treated and untreated populations, but the major effect of ribavirin mutagenesis was to accelerate the occurrence of AU-rich mutant clouds during the early replication rounds of the virus. The standard FMDV quasispecies passaged in the absence of ribavirin included the salient transition-modulating, ribavirin resistance mutation, whose frequency increased in populations treated with ribavirin. Thus, even nonmutagenized FMDV quasispecies include a deep, mutationally biased portion of sequence space, in support of the view that the virus replicates close to the error threshold for maintenance of genetic information.

Lethal mutagenesis is a new antiviral strategy consisting of driving virus toward extinction due to the occurrence of an excess of mutations during viral replication. Many cell culture and some *in vivo* experiments have provided ample support for the extinction of viruses upon replication in the presence of mutagenic nucleoside analogues (reviewed in references 4, 14, and 32). Quasispecies theory and other theoretical treatments support the concept that enhanced mutagenesis can result in virus extinction (3, 7, 8, 20, 48, 63, 71).

The molecular events that lead to loss of virus infectivity by enhanced mutagenesis are only partially understood, and the possible participation of hypermutated genomes is unknown. Previous experimental and *in silico* studies suggested that under limited mutagenesis a class of defective interfering genomes termed "defectors" can be generated during viral replication and that they can interfere with the replication of standard virus, contributing to extinction (34, 38, 44, 58). These observations add to an increasing wealth of evidence that indicates that opposite complementing or interfering interactions among components of the mutant spectrum of viral quasispecies can be a determinant of relevant viral traits such as fitness and virulence (10, 12, 30, 34, 43, 50, 58, 75; reviewed in reference 57). In this view, when the intensity of the mutagenesis increases, overt lethality supersedes interfering interactions, leading to the replicative collapse of the virus. According to the experimental results, the main determinants of viral extinction are the intensity of mutagenesis, low viral load, and low viral fitness (2, 52, 55, 65). Elucidation of the molecular events that underlie virus extinction by lethal mutagenesis has been hampered by the limited number of genomes that can be sequenced from a viral quasispecies by the standard molecular cloning and Sanger sequencing procedures. Only the most frequent mutant genomes are sampled, and minority genomes whose nucleotide sequence may deviate from the consensus sequence or that may contain biased mutation types (hypermutated genomes) go unnoticed. The absence of hypermutated genomes has been taken as evidence against a meltdown of genetic information and as a disproof of error catastrophe (67).

One of the model systems used to study lethal mutagenesis has involved the picornavirus foot-and-mouth disease virus (FMDV) and the mutagenic nucleoside analogue ribavirin (1-β-D-ribofuranosyl-1-*H*-1,2,4-triazole-3-carboxamide) (reviewed in reference 17). Ribavirin could drive FMDV toward extinction during virus replication in cell culture, and extinction was accompanied by an increase in the frequency of G→A and C→U transitions (1, 2, 54, 64). An increase in the mutation frequency of G→A and C→U relative to other transition types was relevant to viral extinction, as suggested by the isolation of a ribavirin-resistant FMDV triple-polymerase mutant (that included substitutions P44S, P169S, and M296I) whose major phenotype is to avoid an excess of G→A and C→U transitions without modification of the average muta-

* Corresponding author. Mailing address: Unité de Rétrovirologie Moléculaire, Institut Pasteur, 28 Rue du Dr. Roux, 75724 Paris Cedex 15, France. Phone: 33 1 44 38 94 45. Fax: 33 1 45 68 88 74. E-mail: jean-pierre.vartanian@pasteur.fr.

† Supplemental material for this article may be found at http://jvi.asm.org/.

▽ Published ahead of print on 14 September 2011.

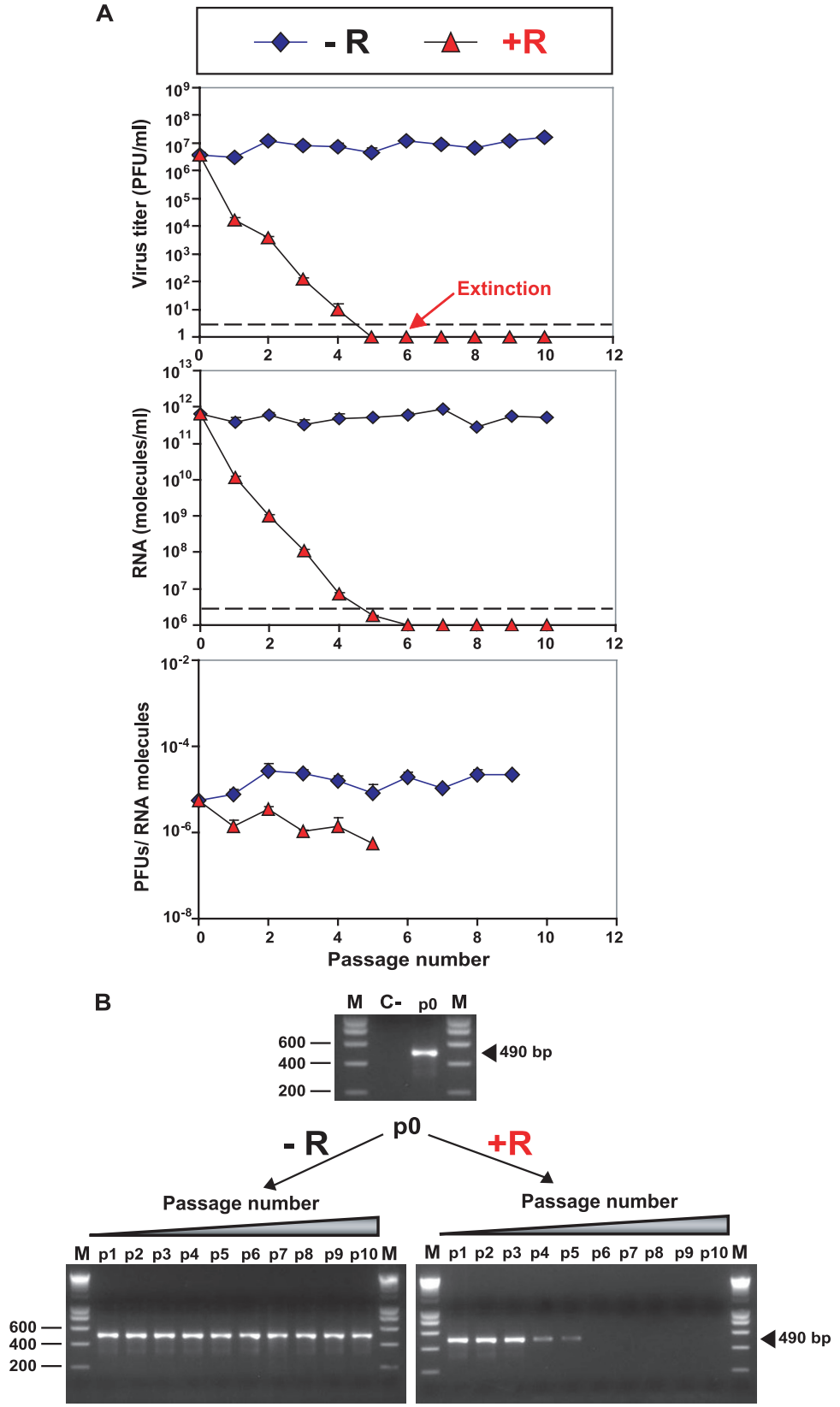

FIG. 1. Extinction of FMDV by ribavirin. A total of 2×10^6 BHK-21 cells were infected with the FMDV WT (progeny of pMT28 transcripts, termed p0; see Materials and Methods) at a multiplicity of infection (MOI) of about 0.3 PFU/cell. For successive passages, the same number of cells was infected with 200 μl of the supernatant from the previous passage. (A) Infectivity, viral RNA molecules, and specific infectivity in the

tion frequency (1). The critical amino acid substitution that suppressed the occurrence of the excess G→A and C→U transitions promoted by ribavirin was P44S, which affects a highly conserved P residue located at a loop between β2 and α2 of the FMDV polymerase (1, 26). In the absence of this substitution, replication in the presence of ribavirin gives rise to deleterious G→A and C→U transitions, including stop codons (1). How the critical mutation that leads to the P44S extinction-escape substitution became dominant in the mutant spectrum of FMDV passaged in the presence of ribavirin is not known.

Here we report the selective amplification by differential DNA denaturation PCR (3D-PCR) and nucleotide sequencing of AU-rich genomes in FMDV populations passaged in the absence or the presence of ribavirin. Both populations included a broad repertoire of hypermutated genomes, and the main consequence of ribavirin mutagenesis was to enhance the biased, hypermutated repertoire at early stages of viral replication with the presence of genomes harboring lethal mutations. Penetration into minority components of the mutant spectrum has also revealed that substitution P44S in the FMDV polymerase was represented in the FMDV quasispecies not subjected to ribavirin mutagenesis and increased in frequency as the population was confronted with ribavirin. The results have unveiled a hitherto unknown complexity of a viral mutant spectrum subjected or not subjected to mutagenesis and the presence of hypermutated viral genomes during transition toward extinction.

MATERIALS AND METHODS

Cells and viruses. The origin of BHK-21 cells and procedures for cell growth in Dulbecco's modified Eagle's medium (DMEM) and for plaque assays in semisolid agar medium have been previously described (16, 66). The viruses used in the experiments are as follows. FMDV C-S8c1 is a plaque-purified derivative of serotype C isolate C1 Santa Pau-Sp70 (66). An infectious clone of FMDV C-S8c1, termed pMT28, was constructed by inserting cDNA of FMDV C-S8c1 into a pGEM-1 plasmid, as described previously (28, 72). Thus, FMDV pMT28 used in the experiments is the progeny of infectious transcripts that express the standard FMDV C-S8c1. To control for the absence of contamination, mock-infected BHK-21 cells were cultured and their supernatants were titrated in parallel with the infected cultures; no signs of infectivity or cytopathology in the cultures or in the control plaque assays were observed in any of the experiments.

Treatment with ribavirin. A solution of ribavirin in phosphate-buffered saline (PBS) was prepared at a concentration of 100 mM, sterilized by filtration, and stored at −70°C. Prior to use, the stock solution was diluted in DMEM to reach the desired ribavirin concentration. For infections in the presence of ribavirin, cell monolayers were pretreated during 7 h with 5 mM ribavirin prior to infection. FMDV C-S8c1 was passaged serially in the absence or presence of ribavirin (5 mM). Incubation of confluent BHK-21 cell monolayers (as used for the infections for FMDV) with 5 mM ribavirin for 31 h resulted in cell viabilities of 40% to 50%, as determined with trypan blue exclusion (range calculated in six different determinations). These values, together with the fact that ribavirin-resistant mutants multiply in BHK-21 cells in the presence of 5 mM ribavirin (1), indicate that toxicity of ribavirin for the cells cannot account for FMDV extinction (54). After addition of FMDV and washing of the cell monolayers, the infection was allowed to proceed in the presence of the same concentration of ribavirin. For each passage, 2×10^6 BHK-21 cells were infected with supernatant of virus from the previous passage (0.2 ml), and the infection continued for about 24 h. The multiplicities of infection (MOI) ranged from 5×10^{-6} to 1×10^{-1} PFU/cell, and the MOI for each passage can be calculated from the infectivity values given for each experiment (Fig. 1). Infections in the absence of ribavirin and mock-infected cells were maintained in parallel; no evidence of contamination of cells with virus was observed at any time.

Assessment of FMDV extinction. FMDV was considered extinct when no virus infectivity was detected and no viral RNA was amplified employing a highly sensitive reverse transcription-PCR (RT-PCR) protocol, either from the supernatant of the cell culture that harbors the putatively extinguished virus or after 3 blind passages of the cell culture supernatants in BHK-21 cells in the absence of any drug. Multiple highly sensitive RT-PCR amplification reactions that yield short cDNAs were carried out to ascertain extinction. These criteria to consider FMDV extinct are those that we have previously described (2, 52, 53, 64, 65). It should be noted that infectivity below the level of detection did not necessarily imply extinction (Fig. 1).

Transcription of viral RNA. Plasmid pMT28 DNA was linearized by cleavage with the appropriate restriction enzymes as previously described (58). Then the plasmid was purified by Wizard PCR Preps DNA purification resin (Promega) and dissolved in RNase-free water. FMDV RNA was transcribed from the linearized plasmid by using the Riboprobe *in vitro* transcription system (Promega). The mixture contained transcription buffer (Promega), 10 mM dithiothreitol, 0.48 U/μl RNasin, 1 mM (each) the standard ribonucleoside triphosphates, 4 ng/μl linearized plasmid DNA, and 0.3 or 0.4 U/μl SP6 or T7 RNA polymerase; it was incubated for 2 h at 37°C. The RNA concentration was estimated by agarose gel electrophoresis, with known amounts of rRNA as a marker.

RNA extraction and quantification of FMDV RNA. Viral RNA was extracted from the medium of infected cells using TRIzol (Invitrogen) as previously described (22). Real-time quantitative RT-PCR was carried out using the Light Cycler RNA Master SYBR green I kit (Roche), according to the instructions of the manufacturer and as described previously for FMDV RNA (22). The 2C coding region was amplified using as primers oligonucleotide 2CR2 (5′-GGCA AACCCTTCAGCAGTAAG; sense orientation [the 5′ nucleotide corresponds to genomic residue 4924]) and oligonucleotide 2CD3 (5′-CGCTCACGTCGAT GTCAAAGTG; antisense orientation [the 5′ nucleotide corresponds to genomic residue 5047]). Quantification was relative to a standard curve obtained with known amounts of FMDV RNA, synthesized by *in vitro* transcription of FMDV cDNA (plasmid pMT28). The specificity of the reaction was monitored by determining the denaturation curve of the amplified DNAs. Negative controls (without template RNA and RNA from mock-infected cells) were run in parallel with each amplification reaction, to ascertain the absence of contamination with undesired templates.

PCR amplification, cloning, and sequencing. Reverse transcription was performed with murine leukemia virus (MLV) reverse transcriptase (Invitrogen), as specified by the manufacturer. Mutated genomes were recovered using differential DNA denaturation PCR (3D-PCR) in a two-round procedure. The first round involved standard amplification: the reaction parameters were 95°C for 5 min, followed by 35 cycles of 95°C for 1 min, 55°C for 30 s, and 72°C for 30 s, and finally 10 min at 72°C. Residues 6610 to 7071 of the polymerase coding region were amplified using as primers oligonucleotide A2SacI (5′-CACACATCGAC CCTGAACCGCACCACGA; sense orientation [the 5′ nucleotide corresponds to genomic residue 6581]) and oligonucleotide AV4 (5′-TTCTCTTTTCTCCA TGAGCTT; antisense orientation [the 5′ nucleotide corresponds to genomic residue 7071]). Amplification products were analyzed by agarose gel electrophoresis using Smart Ladder DNA (Eurogentec) as the molar mass standard. Neg-

supernatants of BHK-21 cells infected with FMDV WT, in the absence (−R) or presence (+R) of ribavirin (5 mM). Titrations and measurements of FMDV RNA by quantitative RT-PCR were carried out in triplicate, and mean values are given. The horizontal discontinuous lines indicate the limit of the detection of infectivity and viral RNA. Procedures for titration of virus infectivity and quantification of FMDV RNA, criteria to consider FMDV extinct, and the positive and negative controls included in the assays are described in Materials and Methods. (B) RT-PCR amplifications used to detect viral RNA in the cell culture supernatants to monitor virus extinction. The treatment with ribavirin and passage number are indicated. The presence or absence of a visible band of 490 bp after RT-PCR amplification indicates extinction (no band) or not (presence of the band). M, molecular size markers (Smart Ladder DNA [Eurogentec], with the corresponding size in base pairs indicated on the left). C−, negative control, amplification without RNA. Conditions of the infections, mutagenic treatment, determination of infectivity, quantification of FMDV RNA, and RT-PCR amplification are detailed in Materials and Methods.

ative controls (amplifications in the absence of RNA) were included in parallel to ascertain absence of contamination by template nucleic acids.

3D-PCR was performed in the second round of amplification using the equivalent of 0.1 μl of the first-round reaction mixture as input. It was carried out using an Eppendorf gradient Mastercycler S programmed to generate 6°C and 2.6°C gradients in the denaturation temperature. The gradient cycler conditions were from 84°C to 90°C for 5 min, followed by 35 cycles of 84°C to 90°C for 1 min, 50°C for 30 s, and 72°C for 30 s, and finally 10 min at 72°C. Residues 6610 to 6839 of the polymerase coding region were amplified using as primers oligonucleotide 5′3D (5′-GGGTTGATCGTTGATACCAGAGA; sense orientation [the 5′ nucleotide corresponds to genomic residue 6610]) and oligonucleotide AV8 (5′-C AGCGGCGGAACAGCGCT; antisense orientation [the 5′ nucleotide corresponds to genomic residue 6839]). The first round gave a 490-bp product, while the second round yielded a 229-bp fragment. The enzyme used for PCR and the 3D-PCR amplification was BioTaq DNA polymerase (Bioline). PCR products were purified from agarose gels and ligated into the TOPO TA cloning vector (Invitrogen, France). After transformation of Top10 Blue cells, up to 50 clones were analyzed. Sequencing was performed using BigDye Terminator V1.1 (Applied Biosystems).

RESULTS

Diving into the mutant spectrum of FMDV by selective amplification of minority genomes. A recently developed procedure that can be applied to the isolation and sequencing of components of a mutant spectrum is differential DNA denaturation PCR (3D-PCR) (70). It consists of the selective amplification of AU-rich genomic RNA mutants by modulating the denaturation temperatures (T_d) during PCR amplification. 3D-PCR has been successfully used to retrieve AU- or AT-rich molecules from viral or cellular genome populations (68–70, 74), in particular in the amplification of G→A hypermutants (24, 29, 36, 59, 61, 70, 73, 74).

Passage of FMDV in BHK-21 cells in the presence of 5 mM ribavirin led to a decrease of virus titer and viral RNA molecules that resulted in diminished specific infectivity and virus extinction at passage 6 (p6) (Fig. 1A). Extinction was evidenced by loss of infectivity and of viral RNA amplifiable by RT-PCR under standard amplification conditions, which were not recovered upon blind passage of the virus in the absence of the drug (1, 54, 56) (Fig. 1B). To analyze the mutant spectrum of FMDV with regard to genomes enriched in AU as a result of the mutagenic activity of ribavirin, the FMDV populations at passages 0 to 5 (p0 to p5, respectively) in the absence or presence of ribavirin were subjected to 3D-PCR. A DNA copy (plasmid pMT28, which expresses wild-type FMDV) (72) and RNA from the initial virus population (p0) were used to determine the denaturation temperature (T_d) range at which residues 6610 to 6839—which encode amino acids 1 to 77 of the viral polymerase and thus include the critical ribavirin-resistance substitution P44S—could be amplified, yielding an amplification product of 229 bp (numbering of genomic residues according to reference 21). The tests (described in Materials and Methods) showed that a T_d of 89.7°C was the minimal T_d that yielded a positive amplification with RNA from the initial FMDV population (Fig. 2A). In the absence of ribavirin, amplification at lower temperatures was observed (from band 0 at 89.7°C at p0 to bands 2b to 5b at 88.4°C at passages 2 to 5, respectively) (Fig. 2A and B). A T_d of 88.4°C was the minimal temperature that yielded a positive 3D-PCR amplification band using as template FMDV RNA from the viral populations passaged either in the absence or presence of ribavirin (Fig. 2B, DNA bands labeled with b). Interestingly, in the presence of ribavirin, an amplification band was obtained at 88.4°C at p1, but not at subsequent passages, suggesting that a class of low-melting-temperature DNA was present after one passage in the presence of ribavirin, but not at later passages (compare bands labeled in red in Fig. 2B, and the overall pattern of amplifications in Fig. 2C).

Nucleotide sequences reveal a dynamics of hypermutated sequences. To determine the nucleotide sequence of the FMDV polymerase coding region in the RNA that was amplified by 3D-PCR, DNA from bands 0, 1a to 5a, and 2b to 5b (which correspond to populations passaged in the absence of ribavirin) and bands 1a to 5a and 1b (which correspond to populations passaged in the presence of ribavirin) (Fig. 2B) were subjected to molecular cloning and sequencing. For the initial FMDV population (p0), the analysis was performed with the DNA amplified with a T_d of 89.7°C (Fig. 2A). The characterization of the populations passaged in the absence of ribavirin indicated an increase of mutation frequency and Shannon entropy of the DNAs with T_d of 88.4°C relative to DNAs with a T_d of 89.1°C for passages 2, 3, and 4 (Table 1). These increases were statistically significant for passages 2, 3, and 4 ($P < 0.0001$, χ^2 test). The maximum mutation frequency was attained at passage 4 and reached 13.1×10^{-3} substitutions per nucleotide (nt). At passage 5, the DNA amplified at both T_d showed a similar mutant spectrum complexity. In the cases in which an increase of complexity at the low T_d was observed, it was associated with a statistically significant increase of the frequency of transitions G→A and C→U ($P < 0.0001$, χ^2 test) (Table 1).

The characterization of the populations passaged in the presence of ribavirin yielded a totally different picture (Table 2). A DNA amplified with a T_d of 88.4°C was obtained for passage 1, but not for subsequent passages (Fig. 2B). The maximum mutant spectrum complexity was attained at this passage and temperature, again with a statistically significant increase of transitions G→A and C→U over other mutation types ($P < 0.0001$, χ^2 test). The presence of a band amplified with a T_d of 88.4°C from RNA at passage 1 and its absence in subsequent passages suggest an initial increased expansion of sequence space toward genomes enriched in AU and a subsequent modification of the mutant spectrum away from such a portion of sequence space (Table 2).

The mutational spectrum of the different populations (Fig. 3) suggests diversification of the AU-rich region of sequence space upon passage of FMDV in the absence of ribavirin (absence of a band at T_d of 88.4°C at passage 1 and comparable complexity of DNA with T_d of 88.4°C and 89.1°C at passage 5). The distribution of mutations per clone (Fig. 4) indicates that at T_d of 88.4°C, most clones include two or more mutations, and at a T_d of 89.1°C, the highest number of mutations per clone was observed at passage 5. In contrast, upon passage in the presence of ribavirin, the initial but transient expansion of the mutant spectrum is reflected in the absence of amplification bands at a T_d of 88.4°C at passages 2, 3, 4, and 5 (Fig. 3). However, genomes harboring 5, 6, and 8 mutations in the polymerase genomic region under analysis (which represent mutation frequencies of 2.6×10^{-2}, 3.1×10^{-2}, and 4.2×10^{-2} substitutions/nt, respectively) were found only in the population at passage 3 but not at early passages (Fig. 4B). The DNAs

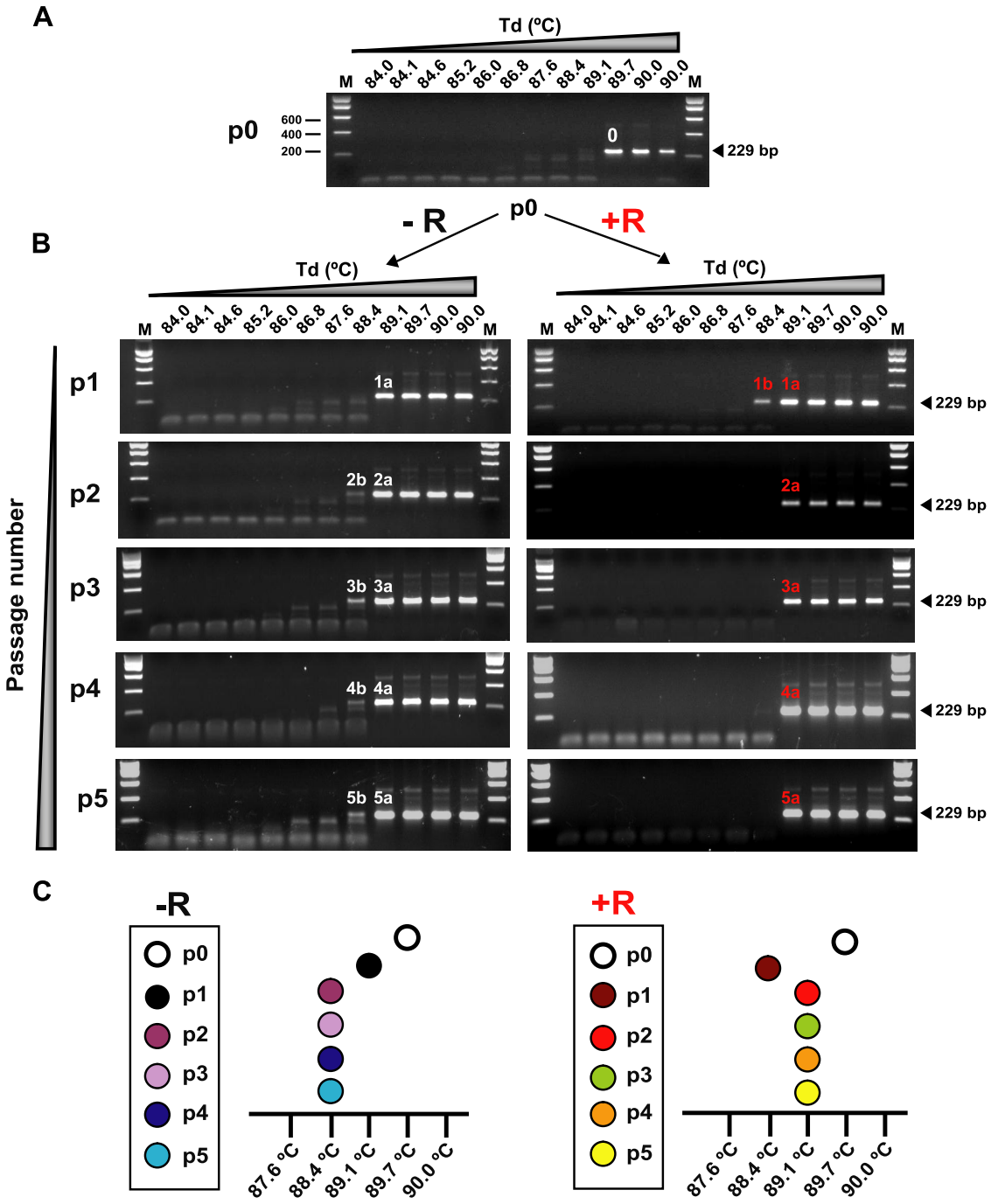

FIG. 2. Amplification of FMDV RNA by 3D-PCR at different denaturation temperatures. (A) 3D-PCR amplification of RNA from FMDV at p0 using the indicated denaturation temperatures (T_d) spanning a 6°C interval (from 84.0°C to 90.0°C); 0 indicates the minimum temperature at which a band of the expected size (229 bp) was obtained. (B) 3D-PCR amplification using the indicated T_d (from 84.0°C to 90.0°C) and RNA from the FMDV populations at passages 1 to 5, in the absence (−R) or presence (+R) of 5 mM ribavirin. M, molecular size markers as described in the legend to Fig. 1. DNA sizes in base pairs are indicated on the right. p followed by a number indicates the passage number. The DNA bands amplified at the indicated temperatures are labeled with a number that corresponds to the passage number followed by a or b. They have been used for further analysis, as described in the text. (C) Schematic representation of the results shown in panel B for easier identification of the positive amplifications at different temperatures and passage number. Procedures for RNA extraction and 3D-PCR are described in Materials and Methods.

obtained with a T_d of 89.1°C (bands 1a to 5a in the "plus ribavirin" branch of Fig. 2B) were reamplified using a T_d range of 86.4°C to 89.0°C (Fig. 5). The presence or absence of an amplification DNA band and the distribution of mutation types show a unique population of genomes selectively amplified at T_d of 86.8°C and 87.3°C for the population passaged 3 times in the presence of ribavirin (Fig. 5 and 6; see Tables S5 and S6 in the supplemental material). The

TABLE 1. Characterization of the mutant spectra represented in the DNA amplified from FMDV populations passaged in the absence of ribavirin

Parameter	Result at passage no. and T_d[a] shown[b]									
	p0 (89.7°C)	p1		p2		p3		p4		p5	
		88.4°C	89.1°C	88.4°C	89.1°C	88.4°C	89.1°C	88.4°C	89.1°C	88.4°C	89.1°C
No. of clones[c]	49		60	41	58	40	55	29	56	38	40
No. of nt[d]	10,584		11,340	7,749	10,962	7,560	10,395	5,481	10,584	7,182	7,560
No. of mutations[e]	49		68	74	25	73	28	73	31	71	73
Mutation frequency[f]	4.6×10^{-3}		5.9×10^{-3}	9.5×10^{-3}	2.2×10^{-3}	9.6×10^{-3}	2.6×10^{-3}	13.1×10^{-3}	2.9×10^{-3}	9.4×10^{-3}	9.6×10^{-3}
Shanon entropy value[g]	0.71		0.8	1.00	0.39	1.00	0.53	1.00	0.48	1.00	1.00
No. (%) of substitutions vs. C-S88c1[h]											
G→A	13 (26)		17 (25)	22 (29)	5 (20)	21 (28)	5 (17)	21 (28)	13 (41)	17 (39)	21 (28)
C→U	21 (42)		22 (32)	26 (35)	4 (16)	30 (41)	4 (14)	29 (39)	6 (19)	29 (40)	30 (41)
Others	15 (30)		29 (42)	26 (35)	16 (64)	22 (30)	19 (67)	23 (31)	12 (38)	25 (35)	22 (30)
No. (%) of substitutions[i]											
Synonymous	19 (38)		28 (41)	19 (25)	5 (20)	18 (24)	8 (28)	22 (30)	8 (25)	25 (35)	18 (24)
Nonsynonymous	30 (61)		40 (58)	55 (74)	20 (80)	55 (75)	20 (71)	51 (69)	23 (74)	46 (64)	55 (75)
No. of synonymous/nonsynonymous substitutions found											
Synonymous[j]											
G→A	7		9	6	0	4	2	5	2	3	4
C→U	10		10	10	2	12	2	12	2	12	12
Others	2		9	3	3	2	4	5	4	10	2
Nonsynonymous[k]											
G→A	6		8	16	5	17	2	16	11	14	17
C→U	11		12	16	2	18	2	17	4	15	20
Others	13		20	23	13	20	16	18	8	17	18

[a] Denaturation temperature at which the mutant spectra were obtained.
[b] The FMDV populations and amplified DNAs are those described in Fig. 2 to 4 in the absence of ribavirin.
[c] Number of molecular clones analyzed (as detailed in Materials and Methods).
[d] Number of nucleotides sequenced.
[e] Number of different mutations found comparing the sequence of each clone with the corresponding sequence of FMDV C-S8c1 (28, 72).
[f] Mutation frequency (number of different mutations found divided by the number of nucleotides sequenced) expressed as number of substitutions per nucleotide. Results are based on the sequencing of 29 to 60 clones per population.
[g] The normalized Shannon entropy is calculated as $-\Sigma_i[(p_i \times \ln p_i)/\ln N]$, in which p_i is the frequency of each sequence in the mutant spectrum and N is the total number of sequences compared.
[h] Number of different G→A, C→U, or other substitutions found comparing the sequence of each clone with the corresponding sequence of FMDV C-S8c1.
[i] Total number of different synonymous and nonsynonymous substitutions.
[j] Number of different synonymous G→A, C→U, or other substitutions, comparing the sequence of each clone with the corresponding sequence of FMDV C-S8c1.
[k] Number of different nonsynonymous G→A, C→U, or other substitutions, comparing the sequence of each clone with the corresponding sequence of FMDV C-S8c1.

TABLE 2. Characterization of the mutant spectra represented in the DNA amplified from FMDV populations passaged in the presence of ribavirin

Parameter	Result at passage no. and T_d[a] shown[b]									
	p0 (89.7°C)	p1		p2		p3		p4		p5	
		88.4°C	89.1°C	88.4°C	89.1°C	88.4°C	89.1°C	88.4°C	89.1°C	88.4°C	89.1°C
No. of clones[c]	56	52	81	58		57		60		69	
No. of nt[d]	10,584	9,828	15,309	10,962		10,773		11,340		13,041	
No. of mutations[e]	49	92	50	52		83		36		64	
Mutation frequency[f]	4.6×10^{-3}	8.8×10^{-3}	3.2×10^{-3}	4.7×10^{-3}		7.7×10^{-3}		3.1×10^{-3}		4.8×10^{-3}	
Shanon entropy value[g]	0.71	1.00	0.61	0.79		1.00		0.63		0.92	
No. (%) of substitutions vs. C-S88c1[h]											
G→A	13 (26)	32 (34)	11 (22)	17 (32)		23 (27)		9 (25)		16 (25)	
C→U	21 (42)	35 (38)	12 (24)	22 (42)		31 (37)		10 (27)		23 (35)	
Others	15 (30)	25 (27)	27 (54)	13 (25)		29 (34)		17 (47)		25 (39)	
No. (%) of substitutions[i]											
Synonymous	19 (38)	34 (36)	18 (36)	20 (38)		26 (31)		10 (27)		21 (32)	
Nonsynonymous	30 (61)	58 (63)	32 (64)	32 (61)		57 (68)		26 (72)		43 (67)	
No. of synynomous/nonsynonymous substitutions											
Synonymous[j]											
G→A	7	8	5	6		7		3		2	
C→U	10	14	6	10		14		4		12	
Others	2	12	7	4		5		3		7	
Nonsynonymous[k]											
G→A	6	24	6	11		16		6		14	
C→U	11	21	6	12		17		6		11	
Others	13	13	20	9		24		14		18	

[a] Denaturation temperature at which the mutant spectra were obtained.
[b] The FMDV populations and amplified DNAs are those described in Fig. 2 to 4 in the presence of ribavirin.
[c] Number of molecular clones analyzed (as detailed in Materials and Methods).
[d] Number of nucleotides sequenced.
[e] Number of different mutations found comparing the sequence of each individual clone with the corresponding sequence of FMDV C-S8c1 (28, 72).
[f] Mutation frequency (number of different mutations found divided by the number of nucleotides sequenced), expressed as substitutions per nucleotide. Results are based on the sequencing of 52 to 81 clones per population.
[g] The normalized Shannon entropy is calculated as $-\Sigma_i[(p_i \times \ln p_i)/\ln N]$, in which p_i is the frequency of each sequence in the mutant spectrum and N is the total number of sequences compared.
[h] Number of different G→A, C→U, or other substitutions found comparing the sequence of each clone with the corresponding sequence of FMDV C-S8c1.
[i] Total number of different synonymous and nonsynonymous substitutions.
[j] Number of different synonymous G→A, C→U, or other substitutions, comparing the sequence of each clone with the corresponding sequence of FMDV C-S8c1.
[k] Number of different nonsynonymous G→A, C→U, or other substitutions, comparing the sequence of each clone with the corresponding sequence of FMDV C-S8c1.

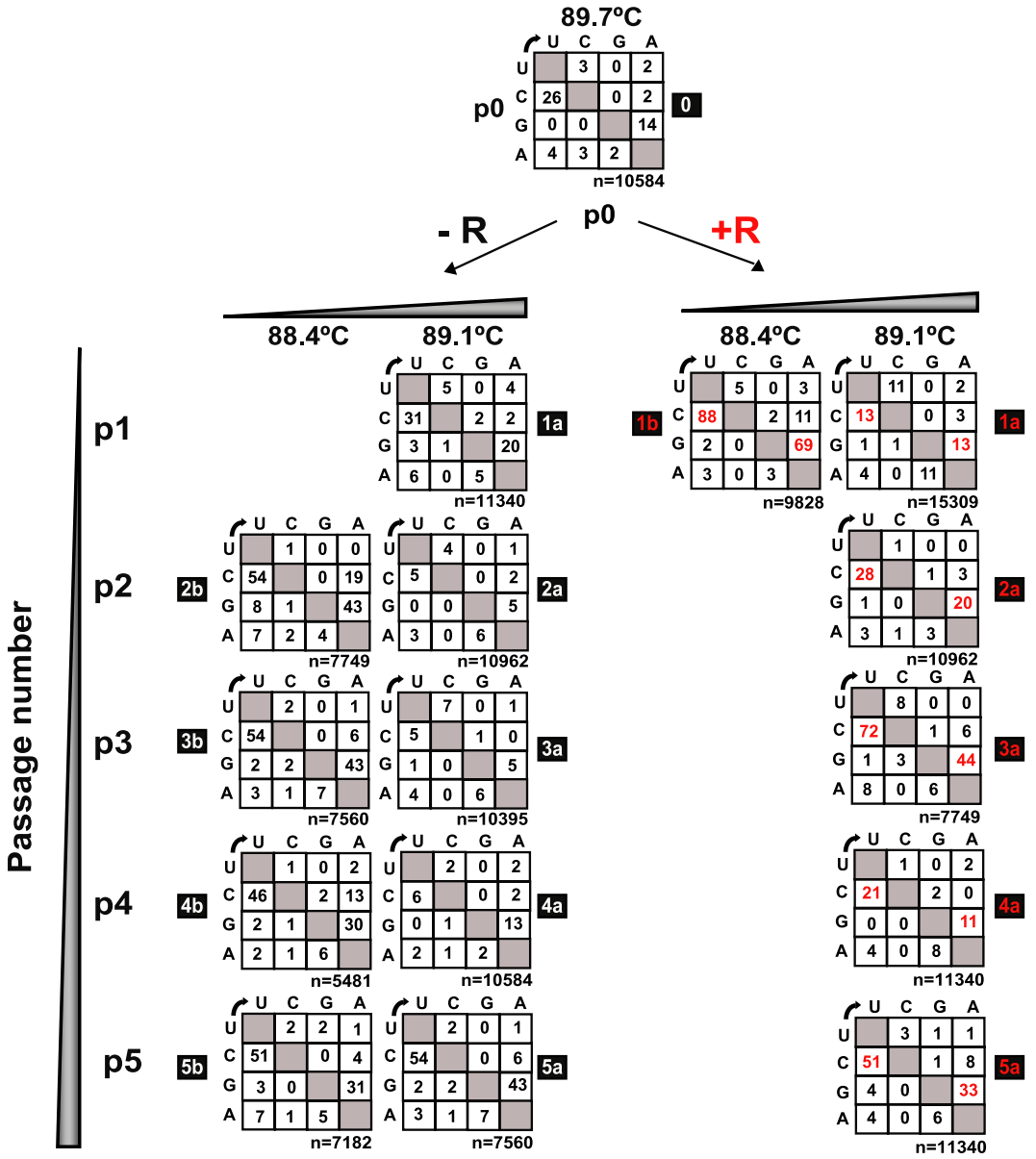

FIG. 3. Types of mutations in the genomes of FMDV populations selectively amplified by 3D-PCR. The passage history of the FMDVs and the amplified DNAs analyzed are given in Fig. 1 and 2A and B. The denaturation temperature used in each 3D-PCR amplification (T_d) is indicated at the top of the boxes; *n* indicates the number of nucleotides sequenced, and p indicates the passage number in either the absence (−R) or presence (+R) of ribavirin. The highlighted numbers and letters next to each box (1a to 5b) correspond to the DNA bands shown in the electrophoreses of Fig. 2B. Lack of a band indicates that no amplification band was detected. The total numbers of nucleotides sequenced were 78,813 for −R and 66,528 for +R. The characterization of the complexity of mutant spectra is summarized in Tables 1 and 2. Procedures for RT-PCR and 3D-PCR amplifications and for nucleotide sequencing are described in Materials and Methods.

analyses indicate a complex, nonlinear variation of mutant spectrum complexity of FMDV populations passaged in the presence of ribavirin.

In contrast to the rescuing of AU-rich genomes by 3D-PCR, a sequence analysis of DNA amplified by standard RT-PCR yielded sequences with a lower frequency of A and U (see Fig. S1 in the supplemental material).

Shifts in mutant repertoire as a result of ribavirin treatment. A critical ribavirin resistance mutation is present in the absence of ribavirin selection. The selective amplification of low-melting-temperature DNA copies of FMDV RNA by virtue of their base composition offered an opportunity to compare the numbers and types of amino acid substitutions in a unique portion of sequence space of FMDV passaged in the absence or presence of ribavirin (Fig. 7A). The complete list of mutations and deduced amino acid substitutions for all populations analyzed (reamplifications excluded) is given in Tables S1 and S2 in the supplemental material for populations passaged in the absence of ribavirin and Tables S3 and S4 in the supplemental material for populations passaged in the presence of ribavirin. Examination of the repertoire of amino acid susbtitutions shows that out of a total of 191 different substi-

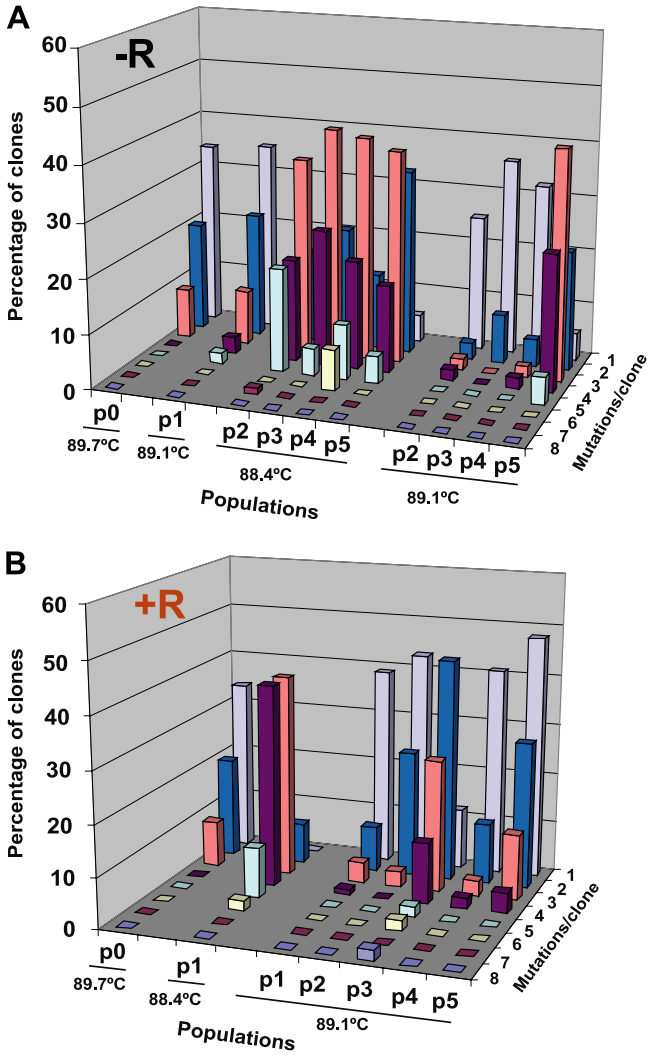

FIG. 4. Overview of the distribution of the number of mutations per molecular clone in the FMDV populations amplified by 3D-PCR. The origin of the populations (p0 to p5) passaged in either the absence (−R) or presence (+R) of ribavirin and amplified DNAs are given in Fig. 1 and 2A and B. The distribution of mutation types is shown in Fig. 3. The front axes identify the FMDV populations and the denaturation temperature (T_d) used for each amplification. Procedures are described in Materials and Methods.

tutions scored, 153 were present in populations passaged in the absence of ribavirin, of which 57 (29.8% of the total) were found exclusively in populations passaged in the absence of ribavirin. A total of 134 amino acid substitutions were present in the populations passaged in the presence of ribavirin, of which 38 (19.9% of the total) were found exclusively in the populations passaged in the presence of ribavirin. Despite the unavoidable limitation in the number of sampled sequences (a total of 145,341 nucleotides from 15 3D-PCR-amplified DNAs), the results show that 50% of the total number of amino acid substitutions in the polymerase are shared by FMDV populations passaged in the absence and presence of ribavirin (see Tables S1 to S4 in the supplemental material). Thus, there is a remarkable overlap in the sequence space occupied in the absence and presence of ribavirin.

Passages in the presence and absence of ribavirin did not result in significant differences regarding the total number of amino acid substitutions relative to the number of nucleotides sequenced (6.8×10^{-3} and 6.2×10^{-3}, respectively) or in the frequency of substitutions with lower, equal, or higher acceptability (i.e., <0, $= 0$, > 0, according to the PAM250 probability matrix [25]) ($P = 0.79$, $P = 0.85$, and $P = 0.72$, respectively; χ^2 test). Interestingly, some amino acid substitutions increased significantly in the presence of ribavirin, including the critical ribavirin resistance substitution P44S (1). P44S was amply represented in the DNA amplified from passage 1 (T_d = 88.4°C, 10 clones; T_d = 89.1°C, 1 clone), passage 2 (T_d = 89.1°C, 1 clone), and passage 3 (T_d = 89.1°C, 6 clones) in the presence of ribavirin (see Tables S3 and S4 in the supplemental material). However, P44S was also present in DNA amplified from populations passaged in the absence of ribavirin at passage 1 (T_d = 89.1°C, 2 clones), passage 3 (T_d = 88.4°C, 3 clones; T_d = 89.1°C, 1 clone), and passage 5 (T_d = 89.1°C, 3 clones) (see Tables S1 and S2 in the supplemental material) (overview in Fig. 7A). The preexistence of ribavirin resistance mutations in populations not treated with ribavirin adds to evidence of the presence of phenotypically relevant mutations in mutant spectra of RNA viruses even in the absence of selection for that phenotype (see Discussion). The quantification of the number of amino acid substitutions as a function of passage number in the absence or presence of ribavirin (Fig. 7B) reflects a dynamics of amino acid changes that mirrors the dynamics of the total mutation types (compare Fig. 3 and 7B). In particular, the increase of genetic complexity at passage 1, which is a hallmark of ribavirin treatment, has a parallel in the number of amino acid substitutions. Thus, the selective amplification of minority FMDV genomes rich in A and U suggests the presence of an ample repertoire of amino acid substitutions, with a significant overlap between populations passaged in the absence and presence of ribavirin, and a disparate evolution of phenotypic space in the absence and presence of ribavirin.

DISCUSSION

The analysis of an AU-rich portion of the genomic sequence space has unveiled a great mutant spectrum complexity not only of FMDV populations passaged in the presence of ribavirin, but also those passaged in its absence. The results confirm the depth of mutant spectra in RNA virus populations in general, previously uncovered using standard molecular and biological cloning, followed by Sanger sequencing, and further evidenced by the recent application of ultradeep sequencing, microarray analysis, or successive amplification methods (13, 18, 27, 41, 45, 57, 76–78).

The present comparison has involved FMDV populations passaged in BHK-21 cells in the absence of ribavirin, that are capable of maintaining the viral genetic information for hundreds of passages (23, 28, 51), and populations passaged in the presence of ribavirin, which are doomed to extinction in a few passages (1, 56). Contrary to expectations, replication in the presence of ribavirin did not result in an overall broader mutant repertoire than that in the absence of ribavirin (compare Fig. 7, Tables 1 and 2, and Tables S1 to S4 in the supplemental material), despite the 3D-PCR targeting AU-rich genomes and being G→A and C→U, the mutation types favored by ribavirin

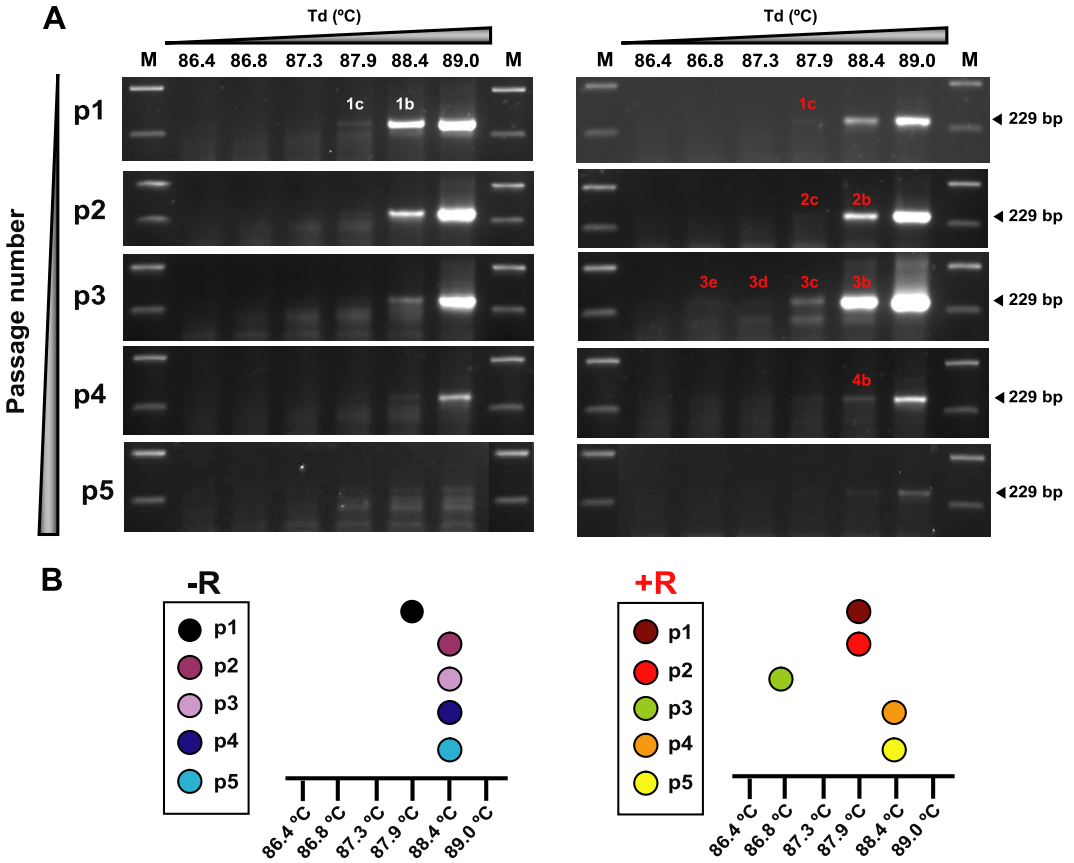

FIG. 5. Reamplification of FMDV RNA by 3D-PCR at different denaturation temperatures. 3D-PCR reamplification at the indicated T_ds (from 86.4°C to 89.0°C), using as template DNA amplified at a T_d of 89.1°C from the populations at passages 1 to 5 in the absence or presence of ribavirin (bands 1a to 5a shown in Fig. 2B). M, molecular size markers as described in the legend to Fig. 1. DNA size in base pairs is indicated on the right. p followed by a number indicates the passage number. The DNA bands amplified at the indicated temperatures are labeled with a number that corresponds to the passage number followed by b, c, d, and e. They have been used for further analysis, as described in the text. (B) Schematic representation of the results shown in panel A with indication of the positive amplifications at different temperatures and passage numbers. Procedures for RNA extraction and 3D-PCR are described in Materials and Methods.

during FMDV replication (1, 2, 56, 64). However, several significant distinctive features of the evolution of the two populations became apparent as a result of the comparison of the T_d values at which a positive amplification was observed, and of the repertoire of mutations in the corresponding populations (compare Fig. 3 in the absence and presence of ribavirin). This amplification asymmetry suggests that the initial infection in the presence of ribavirin produced an expansion in sequence space toward regions rich in A and U that were not represented after one passage in the absence of ribavirin. However, the expanded mutant repertoire could not be maintained despite continuing mutagenesis by ribavirin, presumably due to negative selection acting on highly mutated AU-rich genomes. In favor of this interpretation is a previous study using partition analysis of quasispecies (PAQ) (6) applied to FMDV genomes amplified by RT-PCR under standard conditions, which indicated a compression of the mutant spectrum after multiple passages in the presence of ribavirin, following an initial expansion (49). In the same study, the ratio of nonsynonymous to synonymous mutations suggested the operation of negative selection (49). The deleterious effect of a mutational bias in favor of G→A and C→U was previously evidenced by the fact that the major phenotype of a ribavirin-resistant mutant consisted of an alteration of ribavirin recognition by the FMDV polymerase that prevented the accumulation of genomes with substitutions G→A and C→U (1). The deleterious effect of an excess of substitutions G→A and C→U is in agreement with the limited occupation of this portion of sequence space and the absence of DNA amplification at T_d of 88.4°C at passages 2 through 5 in the presence of ribavirin (Fig. 2). Despite the decline in sequences enriched in AU, sufficient defective genomes promoted by ribavirin must be present in subsequent passages to drive the virus toward extinction (Fig. 1). The analyses have involved residues 9 to 71 of the polymerase coding region. A comparison of the complexity of mutant spectra of different genomic regions of FMDV and other RNA viruses subjected to increased mutagenesis (2, 44, 53, 65) renders it very unlikely that the complexities determined in the polymerase coding region differ substantially for other genomic regions.

The dissimilar evolution of genomic complexity in the absence and presence of ribavirin (Fig. 3) is also observed at the amino acid level (Fig. 7B), suggesting that it may have consequences for phenotypic evolution, in particular due to a nar-

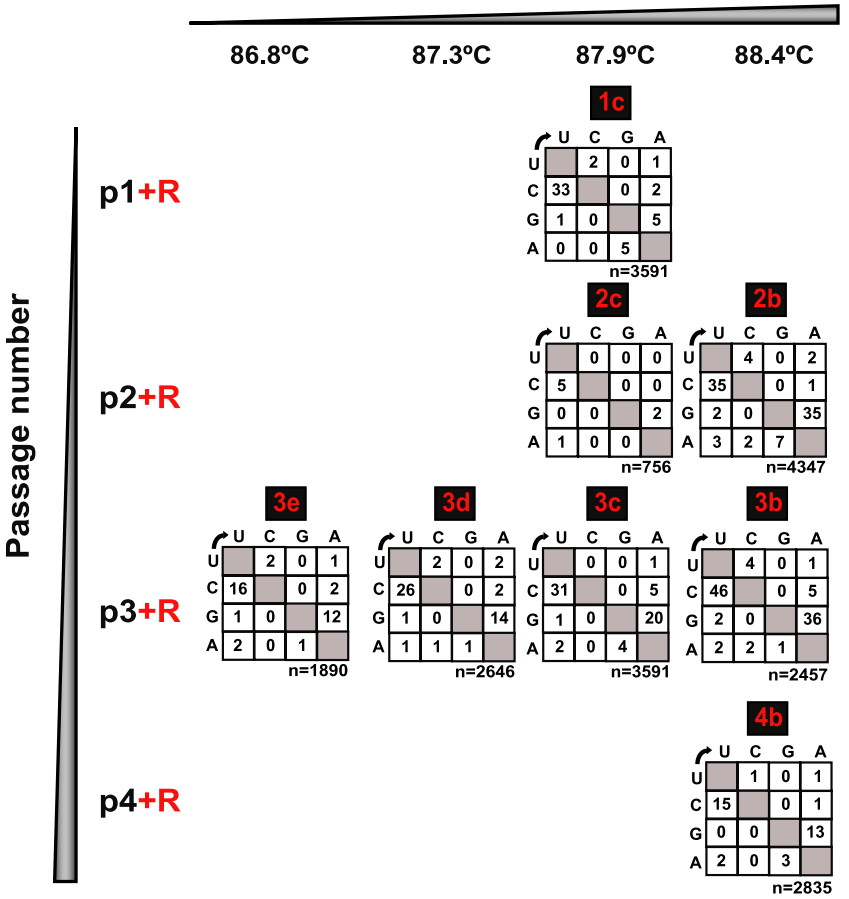

FIG. 6. Types of mutations in the genomes of FMDV populations present in DNA that was reamplified from a specific 3D-PCR product in the presence of ribavirin. The passage history of the FMDVs and the amplified DNAs analyzed are given in Fig. 1 and 5. The denaturation temperature (T_d) used in each 3D-PCR amplification is indicated at the top of the boxes. *n* indicates the number of nucleotides sequenced; p indicates the passage number in the presence (+R) of ribavirin. The highlighted numbers and letters above each box (1c, 2b and 2c, 3b to 3e, and 4b) correspond to the DNA bands shown in the electrophoreses of Fig. 5. Lack of a band indicates that no amplification band was detected. The characterization of the complexity of mutant spectra is summarized in Table S6 in the supplemental material. Procedures for RT-PCR, 3D-PCR amplifications, and nucleotide sequencing are described in Materials and Methods.

rower repertoire of alternative amino acid sequences available for adaptation. This underscores those amino acid substitutions that increased in frequency in the presence of ribavirin, such as P44S, which is responsible for high-level ribavirin resistance in FMDV (1). Substitution P44S does not inflict a detectable fitness cost upon FMDV (1), and this may explain its presence in the mutant spectrum of the virus passaged in the absence of ribavirin. Additional amino acid substitutions within the amino-terminal region of the FMDV polymerase analyzed, which have never been found in consensus sequences or mutant spectra following standard RT-PCR amplification, were detected in the AU-rich subpopulations (Fig. 7; see Tables S1 to S4 in the supplemental material). In addition to P44S, substitutions that were found more than twice in the absence of ribavirin (suggesting there were no severe negative effects on fitness) and that increased to the same or a greater extent than P44S in the presence of ribavirin are P23L > P23S > A38V > P44S (in order of increase in frequency in the presence of ribavirin, based on the data of Fig. 7). Substitutions that followed the same pattern but that were found only twice in the absence of ribavirin are A37V = V51I > P36L > P32S = S40F = E54G (Fig. 7). Also potentially relevant is substitution V55I, found four times in the presence of ribavirin despite V55 being totally invariant in the absence of ribavirin. The substitutions that show the highest increases in the presence of ribavirin are under investigation as possible candidates to confer resistance to ribavirin. In view of the multiple and mechanistically different ribavirin resistance mutations described for picornaviruses (1, 5, 9, 60, 64, 75), it is tempting to speculate that RNA viruses may be endowed with several alternative mutational pathways to achieve ribavirin resistance and that the one chosen depends on the relevant substitutions being present in hidden minorities of mutant spectra due to their low or negligible effect on viral fitness. The presence of the P44S substitution in the mutant spectrum of an FMDV not treated with ribavirin extends previous evidence of the presence of inhibitor resistance mutations in natural viral isolates infecting patients who had never been treated with the corresponding inhibitors (11, 35, 39, 40, 42, 46; reviewed for hepatitis C virus [HCV] in reference 62).

The similar complexity (mutation frequency and Shannon entropy values) scored in the absence and presence of ribavirin

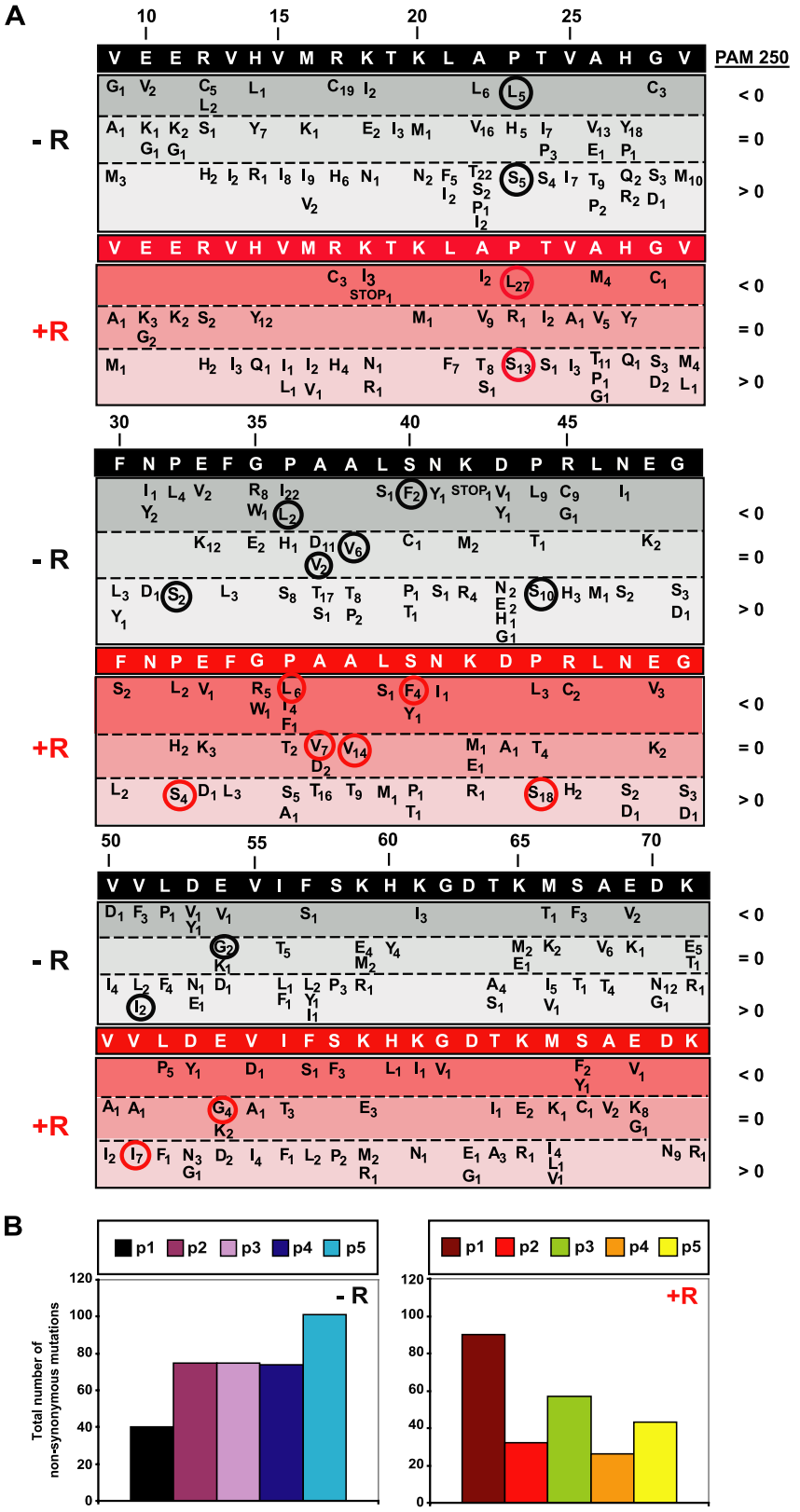

FIG. 7. Amino acid substitutions at the RNA-dependent RNA polymerase region of FMDV amplified by 3D-PCR. (A) All amino acid substitutions deduced from the nucleotide sequences obtained in DNA from the first amplification bands (Fig. 2 and 3 are included). Amino acids 9 to 71 (single-letter code) have been analyzed (sequence in the black box at the top). Amino acid substitutions scored in the absence or presence of ribavirin have been separated based on the probability of occurrence according to the PAM250 substitution matrix (25), where <0, = 0, and >0 in shades of gray and red represent substitutions in the absence (−R) or presence (+R) of ribavirin, respectively. Subindices indicate the number of times that a given amino acid has been found among the viral population analyzed. Amino acids that correspond to substitutions that occurred at least twice in the absence of ribavirin and that increased to the same or a larger extent than P44S in the presence of ribavirin have been circled (see text). (B) Evolution of the total number of amino acid substitutions (i.e., those depicted in panel A) as a function of passage number. Procedures are described in Materials and Methods.

(Tables 1 and 2) reinforces the concept that the virus replicates close to an error threshold for maintenance of genetic information, as previously suggested from independent approaches (15, 19, 20, 37). Although sequence heterogeneities of FMDV within infected animals have been reported (16, 47, 77), it is not known whether natural isolates of the virus display such a broad repertoire of genomes with high AU base frequencies. Despite a claim to the contrary (67), extinction of FMDV by lethal mutagenesis is a new paradigm in antiviral therapy since its basic mechanism is not merely a decrease in viral load and of the R_0 value (defined in reference 8) but a melting of genetic information evoked by mutagenesis that results in a decrease of R_0. The present study has revealed that such a melting is mediated by an early movement in sequence space toward highly mutated genomes that precedes a decrease in viral load and the subsequent extinction. An RNA close to what could classify as hypermutated genome was detected in a previous analysis of lymphocytic choriomeningitis virus (LCMV) subjected to 5-fluorouracil mutagenesis (33). However, a shift in sequence space was not noticed using previous approaches based on standard biological or molecular cloning and sequencing. Movements in sequence space may be a relevant ingredient in the transition toward error catastrophe. An invariant consensus sequence may conceal lethal defection by an early shift in regions of sequence space prone to produce defector genomes (31, 33, 34).

ACKNOWLEDGMENTS

We thank A. I. de Ávila and P. M. Perales for help with the sequence analysis.

This work was supported by grants BFU2008-02816/BMC, Proyecto Intramural de Frontera del CSIC 200820FO191, and FIPSE 36558/06, Fundación Ramón Areces. CIBERehd is funded by Instituto de Salud Carlos III. C.P. is the recipient of a contract from CIBERehd. A stay of C.P. at the Pasteur Institute (Paris) was supported by short-term EMBO fellowship no. 18-2009. This work was supported by grants from the Institut Pasteur and the CNRS. The URM from Institut Pasteur is "Equipe Labelisée LIGUE 2010."

REFERENCES

1. **Agudo, R., et al.** 2010. A multi-step process of viral adaptation to a mutagenic nucleoside analogue by modulation of transition types leads to extinction-escape. PLoS Pathog. **6:**e1001072.
2. **Airaksinen, A., N. Pariente, L. Menendez-Arias, and E. Domingo.** 2003. Curing of foot-and-mouth disease virus from persistently infected cells by ribavirin involves enhanced mutagenesis. Virology **311:**339–349.
3. **Alves, D., and J. F. Fontanari.** 1998. Error threshold in finite populations. Phys. Rev. E **57:**7008–7013.
4. **Anderson, J. P., R. Daifuku, and L. A. Loeb.** 2004. Viral error catastrophe by mutagenic nucleosides. Annu. Rev. Microbiol. **58:**183–205.
5. **Arias, A., et al.** 2008. Determinants of RNA-dependent RNA polymerase (in)fidelity revealed by kinetic analysis of the polymerase encoded by a foot-and-mouth disease virus mutant with reduced sensitivity to ribavirin. J. Virol. **82:**12346–12355.
6. **Baccam, P., R. J. Thompson, O. Fedrigo, S. Carpenter, and J. L. Cornette.** 2001. PAQ: partition analysis of quasispecies. Bioinformatics **17:**16–22.
7. **Biebricher, C. K., and M. Eigen.** 2005. The error threshold. Virus Res. **107:**117–127.
8. **Bull, J. J., R. Sanjuan, and C. O. Wilke.** 2007. Theory of lethal mutagenesis for viruses. J. Virol. **81:**2930–2939.
9. **Castro, C., J. J. Arnold, and C. E. Cameron.** 2005. Incorporation fidelity of the viral RNA-dependent RNA polymerase: a kinetic, thermodynamic and structural perspective. Virus Res. **107:**141–149.
10. **Crowder, S., and K. Kirkegaard.** 2005. Trans-dominant inhibition of RNA viral replication can slow growth of drug-resistant viruses. Nature Genet. **37:**701–709.
11. **Cubero, M., et al.** 2008. Naturally occurring NS3-protease-inhibitor resistant mutant A156T in the liver of an untreated chronic hepatitis C patient. Virology **370:**237–245.
12. **de la Torre, J. C., and J. J. Holland.** 1990. RNA virus quasispecies populations can suppress vastly superior mutant progeny. J. Virol. **64:**6278–6281.
13. **Domingo, E., et al.** 2006. Viruses as quasispecies: biological implications. Curr. Top. Microbiol. Immunol. **299:**51–82.
14. **Domingo, E., (ed.).** 2005. Virus entry into error catastrophe as a new antiviral strategy. Virus Res. **107:**115–228.
15. **Domingo, E., C. Biebricher, M. Eigen, and J. J. Holland.** 2001. Quasispecies and RNA virus evolution: principles and consequences. Landes Bioscience, Austin, TX.
16. **Domingo, E., M. Davila, and J. Ortin.** 1980. Nucleotide sequence heterogeneity of the RNA from a natural population of foot-and-mouth-disease virus. Gene **11:**333–346.
17. **Domingo, E., et al.** 2010. Mutation, quasispecies and lethal mutagenesis, p. 197–211. *In* E. Ehrenfeld, E. Domingo, and R. P. Roos (ed.), The picornaviruses. ASM Press, Washington, DC.
18. **Domingo, E., and S. Wain-Hobson.** 2009. The 30th anniversary of quasispecies. Meeting on 'Quasispecies: Past, Present and Future.' EMBO Rep. **10:**444–448.
19. **Drake, J. W., and J. J. Holland.** 1999. Mutation rates among RNA viruses. Proc. Natl. Acad. Sci. U. S. A. **96:**13910–13913.
20. **Eigen, M.** 2002. Error catastrophe and antiviral strategy. Proc. Natl. Acad. Sci. U. S. A. **99:**13374–13376.
21. **Escarmís, C., et al.** 1996. Genetic lesions associated with Muller's ratchet in an RNA virus. J. Mol. Biol. **264:**255–267.
22. **Escarmís, C., E. Lazaro, A. Arias, and E. Domingo.** 2008. Repeated bottleneck transfers can lead to non-cytocidal forms of a cytopathic virus: implications for viral extinction. J. Mol. Biol. **376:**367–379.
23. **Escarmis, C., C. Perales, and E. Domingo.** 2009. Biological effect of Muller's Ratchet: distant capsid site can affect picornavirus protein processing. J. Virol. **83:**6748–6756.
24. **Fan, J., et al.** 2010. APOBEC3G generates nonsense mutations in human T-cell leukemia virus type 1 proviral genomes in vivo. J. Virol. **84:**7278–7287.
25. **Feng, D. F., and R. F. Doolittle.** 1996. Progressive alignment of amino acid sequences and construction of phylogenetic trees from them. Methods Enzymol. **266:**368–382.
26. **Ferrer-Orta, C., et al.** 2004. Structure of foot-and-mouth disease virus RNA-dependent RNA polymerase and its complex with a template-primer RNA. J. Biol. Chem. **279:**47212–47221.
27. **Garcia-Arriaza, J., E. Domingo, and C. Briones.** 2007. Characterization of minority subpopulations in the mutant spectrum of HIV-1 quasispecies by successive specific amplifications. Virus Res. **129:**123–134.
28. **García-Arriaza, J., S. C. Manrubia, M. Toja, E. Domingo, and C. Escarmís.** 2004. Evolutionary transition toward defective RNAs that are infectious by complementation. J. Virol. **78:**11678–11685.
29. **Gonzalez, M. C., et al.** 2009. Human APOBEC1 cytidine deaminase edits HBV DNA. Retrovirology **6:**96.
30. **González-López, C., A. Arias, N. Pariente, G. Gómez-Mariano, and E. Domingo.** 2004. Preextinction viral RNA can interfere with infectivity. J. Virol. **78:**3319–3324.
31. **González-López, C., G. Gómez-Mariano, C. Escarmís, and E. Domingo.** 2005. Invariant aphthovirus consensus nucleotide sequence in the transition to error catastrophe. Infect. Genet. Evol. **5:**366–374.
32. **Graci, J. D., and C. E. Cameron.** 2008. Therapeutically targeting RNA viruses via lethal mutagenesis. Future Virol. **3:**553–566.
33. **Grande-Pérez, A., G. Gómez-Mariano, P. R. Lowenstein, and E. Domingo.** 2005. Mutagenesis-induced, large fitness variations with an invariant arenavirus consensus genomic nucleotide sequence. J. Virol. **79:**10451–10459.
34. **Grande-Pérez, A., E. Lazaro, P. Lowenstein, E. Domingo, and S. C. Manrubia.** 2005. Suppression of viral infectivity through lethal defection. Proc. Natl. Acad. Sci. U. S. A. **102:**4448–4452.
35. **Havlir, D. V., S. Eastman, A. Gamst, and D. D. Richman.** 1996. Nevirapine-resistant human immunodeficiency virus: kinetics of replication and estimated prevalence in untreated patients. J. Virol. **70:**7894–7899.
36. **Henry, M., et al.** 2009. Genetic editing of HBV DNA by monodomain human APOBEC3 cytidine deaminases and the recombinant nature of APOBEC3G. PLoS One **4:**e4277.
37. **Holland, J. J., E. Domingo, J. C. de la Torre, and D. A. Steinhauer.** 1990. Mutation frequencies at defined single codon sites in vesicular stomatitis virus and poliovirus can be increased only slightly by chemical mutagenesis. J. Virol. **64:**3960–3962.
38. **Iranzo, J., and S. C. Manrubia.** 2009. Stochastic extinction of viral infectivity through the action of defectors. Europhysics Lett. **85:**18001.
39. **Johnson, J. A., et al.** 2008. Minority HIV-1 drug resistance mutations are present in antiretroviral treatment-naive populations and associate with reduced treatment efficacy. PLoS Med. **5:**e158.
40. **Kuntzen, T., et al.** 2008. Naturally occurring dominant resistance mutations to hepatitis C virus protease and polymerase inhibitors in treatment-naive patients. Hepatology **48:**1769–1778.
41. **Lauring, A. S., and R. Andino.** 2011. Exploring the fitness landscape of an RNA virus by using a universal barcode microarray. J. Virol. **85:**3780–3791.
42. **Lech, W. J., et al.** 1996. In vivo sequence diversity of the protease of human

immunodeficiency virus type 1: presence of protease inhibitor-resistant variants in untreated subjects. J. Virol. **70:**2038–2043.
43. **Levi, L. I., et al.** 2010. Fidelity variants of RNA dependent RNA polymerases uncover an indirect, mutagenic activity of amiloride compounds. PLoS Pathog. **6:**e1001163.
44. **Martin, V., D. Abia, E. Domingo, and A. Grande-Perez.** 2010. An interfering activity against lymphocytic choriomeningitis virus replication associated with enhanced mutagenesis. J. Gen. Virol. **91:**990–1003.
45. **Mas, A., C. Lopez-Galindez, I. Cacho, J. Gomez, and M. A. Martinez.** 2010. Unfinished stories on viral quasispecies and Darwinian views of evolution. J. Mol. Biol. **397:**865–877.
46. **Nájera, I., et al.** 1995. Pol gene quasispecies of human immunodeficiency virus: mutations associated with drug resistance in virus from patients undergoing no drug therapy. J. Virol. **69:**23–31.
47. **Nunez, J. I., et al.** 2007. Guinea pig-adapted foot-and-mouth disease virus with altered receptor recognition can productively infect a natural host. J. Virol. **81:**8497–8506.
48. **Ochoa, G.** 2006. Error thresholds in genetic algorithms. Evol. Comput. **14:** 157–182.
49. **Ojosnegros, S., et al.** 2008. Topology of evolving, mutagenized viral populations: quasispecies expansion, compression, and operation of negative selection. BMC Evol. Biol. **8:**207.
50. **Ojosnegros, S., et al.** 2010. Competition-colonization dynamics in an RNA virus. Proc. Natl. Acad. Sci. U. S. A. **107:**2108–2112.
51. **Ojosnegros, S., et al.** 2011. Viral genome segmentation can result from a trade-off between genetic content and particle stability. PLoS Genet. **7:**e1001344.
52. **Pariente, N., A. Airaksinen, and E. Domingo.** 2003. Mutagenesis versus inhibition in the efficiency of extinction of foot-and-mouth disease virus. J. Virol. **77:**7131–7138.
53. **Pariente, N., S. Sierra, P. R. Lowenstein, and E. Domingo.** 2001. Efficient virus extinction by combinations of a mutagen and antiviral inhibitors. J. Virol. **75:**9723–9730.
54. **Perales, C., R. Agudo, and E. Domingo.** 2009. Counteracting quasispecies adaptability: extinction of a ribavirin-resistant virus mutant by an alternative mutagenic treatment. PLoS One **4:**e5554.
55. **Perales, C., R. Agudo, S. C. Manrubia, and E. Domingo.** 2011. Influence of mutagenesis and viral load on the sustained low-level replication of an RNA virus. J. Mol. Biol. **407:**60–78.
56. **Perales, C., R. Agudo, H. Tejero, S. C. Manrubia, and E. Domingo.** 2009. Potential benefits of sequential inhibitor-mutagen treatments of RNA virus infections. PLoS Pathog. **5:**e1000658.
57. **Perales, C., R. Lorenzo-Redondo, C. López-Galíndez, M. A. Martínez, and E. Domingo.** 2010. Mutant spectra in virus behavior. Future Virol. **5:**679–698.
58. **Perales, C., R. Mateo, M. G. Mateu, and E. Domingo.** 2007. Insights into RNA virus mutant spectrum and lethal mutagenesis events: replicative interference and complementation by multiple point mutants. J. Mol. Biol. **369:**985–1000.
59. **Petit, V., et al.** 2009. Murine APOBEC1 is a powerful mutator of retroviral and cellular RNA in vitro and in vivo. J. Mol. Biol. **385:**65–78.
60. **Pfeiffer, J. K., and K. Kirkegaard.** 2003. A single mutation in poliovirus RNA-dependent RNA polymerase confers resistance to mutagenic nucleotide analogs via increased fidelity. Proc. Natl. Acad. Sci. U. S. A. **100:**7289–7294.
61. **Renard, M., M. Henry, D. Guétard, J. P. Vartanian, and S. Wain-Hobson.** 2010. APOBEC1 and APOBEC3 cytidine deaminases as restriction factors for hepadnaviral genomes in non-humans in vivo. J. Mol. Biol. **400:**323–334.
62. **Sarrazin, C., and S. Zeuzem.** 2010. Resistance to direct antiviral agents in patients with hepatitis C virus infection. Gastroenterology **138:**447–462.
63. **Schuster, P., and P. Stadler.** 2008. Early replicons: origin and evolution, p. 1–41. *In* E. Domingo, C. Parrish, and J. J. Holland (ed.), Origin and evolution of viruses. Elsevier, Philadelphia, PA.
64. **Sierra, M., et al.** 2007. Foot-and-mouth disease virus mutant with decreased sensitivity to ribavirin: implications for error catastrophe. J. Virol. **81:**2012–2024.
65. **Sierra, S., M. Dávila, P. R. Lowenstein, and E. Domingo.** 2000. Response of foot-and-mouth disease virus to increased mutagenesis. Influence of viral load and fitness in loss of infectivity. J. Virol. **74:**8316–8323.
66. **Sobrino, F., M. Dávila, J. Ortín, and E. Domingo.** 1983. Multiple genetic variants arise in the course of replication of foot-and-mouth disease virus in cell culture. Virology **128:**310–318.
67. **Summers, J., and S. Litwin.** 2006. Examining the theory of error catastrophe. J. Virol. **80:**20–26.
68. **Suspène, R., et al.** 2011. Somatic hypermutation of human mitochondrial and nuclear DNA by APOBEC3 cytidine deaminases, a pathway for DNA catabolism. Proc. Natl. Acad. Sci. U. S. A. **108:**4858–4863.
69. **Suspène, R., et al.** 2005. Extensive editing of both hepatitis B virus DNA strands by APOBEC3 cytidine deaminases in vitro and in vivo. Proc. Natl. Acad. Sci. U. S. A. **102:**8321–8326.
70. **Suspène, R., M. Henry, S. Guillot, S. Wain-Hobson, and J. P. Vartanian.** 2005. Recovery of APOBEC3-edited human immunodeficiency virus G→A hypermutants by differential DNA denaturation PCR. J. Gen. Virol. **86:**125–129.
71. **Takeuchi, N., and P. Hogeweg.** 2007. Error-threshold exists in fitness landscapes with lethal mutants. BMC Evol. Biol. **7:**15. (Letter.)
72. **Toja, M., C. Escarmis, and E. Domingo.** 1999. Genomic nucleotide sequence of a foot-and-mouth disease virus clone and its persistent derivatives. Implications for the evolution of viral quasispecies during a persistent infection. Virus Res. **64:**161–171.
73. **Vartanian, J. P., D. Guétard, M. Henry, and S. Wain-Hobson.** 2008. Evidence for editing of human papillomavirus DNA by APOBEC3 in benign and precancerous lesions. Science **320:**230–233.
74. **Vartanian, J. P., et al.** 2010. Massive APOBEC3 editing of hepatitis B viral DNA in cirrhosis. PLoS Pathog. **6:**e1000928.
75. **Vignuzzi, M., J. K. Stone, J. J. Arnold, C. E. Cameron, and R. Andino.** 2006. Quasispecies diversity determines pathogenesis through cooperative interactions in a viral population. Nature **439:**344–348.
76. **Webster, D. R., et al.** 2009. An enhanced single base extension technique for the analysis of complex viral populations. PLoS One **4:**e7453.
77. **Wright, C. F., et al.** 2011. Beyond the consensus: dissecting within-host viral population diversity of foot-and-mouth disease virus by using next-generation genome sequencing. J. Virol. **85:**2266–2275.
78. **Zagordi, O., R. Klein, M. Daumer, and N. Beerenwinkel.** 2010. Error correction of next-generation sequencing data and reliable estimation of HIV quasispecies. Nucleic Acids Res. **38:**7400–7409.